



INVESTIGATING THE EFFECT OF INTEGRATION OF RENEWABLE POWER PLANTS ON THE NIGERIA 330KV ELECTRICITY GRID

Martin Abreka E.¹, Peter O. Ohiero², Iyaji Sunday Ogbaji³ and Akonjom Nsed Ayip⁴

^{1, 2, 3} Department of Electrical and Electronic Engineering, University of Cross River State, Calabar, Nigeria

⁴ Department of Physics, University of Cross River State, Calabar, Nigeria

Correspondence email: peterohiero@unicross.edu.ng

Abstract

Nigeria is faced with huge challenge of inadequate power supply and low access to electricity. These have affected the economic and social development of the country. However, Nigeria has abundant renewable (alternative) energy resources that can be exploited through large integration of renewable energy sources. In order to address shortage of electricity supply, the Federal Government of Nigeria awarded the construction of a 10MW solar power plant in Kano State and a 10MW wind power plant in Katsina State. These projects are going to be the first grid connected renewable power plants in the country. The constructions of these projects are in advanced stage but before they are connected to the electricity grid, it is necessary to carry out a study to know the effect they will and their expansion will have on the performance of the grid. In this research, a model of the existing Nigeria 330kV power network was developed in Electrical Transient Analyser Program (ETAP) software which was used to simulate load flow based on Newton Raphson method. Simulations were carried out to analyse the steady state performance of the existing network, the existing network and the 10MW solar plant only, the existing network and the 10MW wind power plant only, the existing network and a combination of 10MW solar and 10MW wind power plants and with increased penetration level of the renewable power plants. In each case, the voltage magnitude and power losses were measured and the weak buses identified and the voltage stability analysed. The results of the current 330kV network without the integration of renewable sources shows buses that have voltages outside the stability limit and the total power losses. When solar or wind power plant and solar and wind power plants were connected to the grid, the voltage increased and the power losses reduced. An average improvement of 3.3% of the voltage magnitude and 4.10% reduction in power losses occurred when both solar and wind power plants were connected to the grid. Also, a study of the maximum penetration level of solar and wind power plants into the grid was conducted. We considered buses where voltage stability limit was violated. Such places include Jos, Kaduna, Kano, Jalingo, Yola, Gombe, Damaturu and Maiduguri. It was observed that as the penetration level increased, the voltage magnitude also increased except that of Kano bus which decreased The maximum penetration of the renewable

**INVESTIGATING THE EFFECT OF INTEGRATION OF RENEWABLE POWER PLANTS ON THE NIGERIA
330KV ELECTRICITY GRID**

Martin, et al.

power plants at Kano and Katsina substations beyond which voltage stability will be violated is 20MW. The results showed improvement in the power generation and voltage magnitude and reduction in power losses. It suggests therefore that voltage compensator is required at the Kano bus to improve the voltage magnitude.

Keywords: Solar, Wind, Load flow, Voltage stability, Power losses

1.0 Introduction

Integration of renewable energy sources into electric power grid is the most promising solution to diversify the sources of energy generation, reduce reliance on fossil fuels, reduce dependence on imported fuels, improve power supply to meet the ever increasing demand for electrical energy, reduce greenhouse gas emission and pollutants and their harmful effect on environment, provide clean and green environment, and increase the power system resilience in order to have a sustainable, reliable, stable, cost effective and efficient electricity system. Renewable energy sources also enable the generators to be located close to the load centres reducing the cost of long transmission lines and line losses. However, incorporating renewable energy sources into existing grid results to planning, technical, management and operational challenges for power system operators due to the variability and intermittency of renewable energy, the need for grid stability, and the demand for high-quality power supply.

When renewable energy sources are integrated into the grid at different parts of the electric power system, the direction and load flow pattern of active and reactive power changes resulting to changes in the voltage and frequency profile as well as losses along the transmission lines. A gradual increase in the level of penetration of the renewable energy sources into the grid will alter the voltage and frequency profile as well as the stability and power quality of the system. It is important to know and quantify the effect the renewable energy sources will have on the existing electric power system in order to proffer

ways to overcome them before wide integration.

Different types of renewable energy resources namely solar, wind, biomass, hydro, etc. can be integrated to the grid. The most promising and widely utilised renewable sources for the generation of electricity is the solar and wind. According to International Energy Agency 2022, solar accounts for 4.5% of the world total electricity generation following wind which made up 7.5% [IEA 2022].

With the improvement in technology, renewable energy set to contribute 80% to the world power generation by 2030 (UN 2022). As a matter of fact, it is reported under the renewable energy road map of Nigeria by IRENA 2023, that the share of renewable energy sources will be 47% of electricity generation in Nigeria by 2030 and 57% by 2050 (IRENA, 2023). Studies over the years revealed that Nigeria has abundant renewable energy sources that can be utilised to meet electricity needs of the country. It has been discovered that the wind speed in the Northern region is between 4.0m/s to 7.5m/s at 10m above ground (Elemo, E.O., Ogobor, E.A., Alagbe, etal, 2021), these wind speed and the average horizontal global radiation are suitable for the generation of electricity.

In an effort to increase supply of electricity, the Federal Government of Nigeria in 2012 awarded contracts for the construction and integration of 10MW wind power plant at Katsina State and 10MW solar power plant in Kano State (Lawa Salisu and Dr. Isa Garba, 2013), these projects are in advanced stage of completion and are yet to be integrated into the grid. It is believed that

after a successful completion of these projects and integration into the grid, they will pave way for a large-scale development and integration to the grid. The successful integration of these power plants (solar and wind) will have both positive and negative effect on the electricity grid and poses challenge. Electricity generators using renewable energy sources can only produce electricity when the weather conditions are favourable. In another way, there are intermittent in nature and fluctuates periodically and as such cannot be dispatched. The intermittent and unpredictability of these categories of energy sources makes it difficult to maintained demand - generation balance under different generation conditions since variable electricity is generated from these sources which may lead to load-generation imbalance, voltage fluctuation, reverse power flow which can affect the stability and security of the grid. Grid integration involves the connection of new power generators into the existing grid. The integration of renewable energy sources also changes the characteristics of power system from a one-way power flow to a two-way power flow which poses challenges in protection (Eissa (SIEEE), M. M, 2015). It requires but not limited to upgrade in the transmission network. This is expensive and may take a long time to achieve. Above all, is the issue of cost and efficiency. The cost however is reducing due to advancements in technology with the efficiency which have not experience reasonable improvement. It is important to understand the complexity of the system network and the effect the renewable energy sources will have on the existing grid and how they contribute to balancing

the electricity supply and demand before the physical integration of the renewable energy sources. Studies of the effect of renewable energy resources has been carried out in many countries that have successfully connected renewable sources to grid, but there is limited information of such study on the Nigeria 330kV network. In order to identify and prevent any problems that may occur during the integration and usage of the solar and wind power plant into the grid, it is necessary to investigate the effect of integration of these renewable energy sources into the Nigeria 330kV grid.

Different authors and researchers have studied the effect of integration of solar and wind power plants on the stability of power system. M. Singh, M. H. V and V. H. S, (2022), investigated on the power system stability with integration of renewable resources, where they conducted a steady state voltage stability analysis for an IEEE39 bus systems under high penetration of solar and wind power. Different operational scenarios with wind, solar and mix of both were studied to investigate the voltage stability issues in this IEEE-39. The simulation work is performed in PSSE software. M. J. Mbunwe and A. O. Ekwue (2020), carried out a voltage stability analysis of the Nigerian Power system using annealing optimization where they conducted a model and simulation of a 28 bus Nsukka 11kV Campus Feeder. They tested their proposed optimized voltage stability index using fast voltage stability indicator minimized by the simulated annealing optimization technique. It was concluded that the conducted application on standard system has satisfactory results for optimal voltage stability level as well as for extending the loading level of the system. In

the work of E.N Ezeruigbo, etal (2021), they analysed the voltage stability of Nigerian 330kV power grid using static P-V Plots but limited their study to the south eastern region of Nigeria. This study further identified vulnerable buses to voltage instability. The study did not consider the effect of solar and wind power plants and the south east network is a part of the entire Nigerian 330kV network and does not reflect the complex interconnection of the Nigerian 330kV network. The Impact of integrating large-scale DFIG-based wind energy conversion system on the voltage stability of weak national grids was conducted by Bukola Babatunde Adetokun, and Christopher Maina Muriithi, (2021). A DFIG-based wind energy conversion system was used to investigate the impact variable wind power generator have on Nigerian electricity grid. The paper concluded DFIG-based WECS as a viable solution for voltage improvement. To close these gaps, this research focused on investigating the effect of solar and wind on voltage stability and power losses as well as determining the maximum penetration levels when all the components of the network are connected together. This study is carried out using Newton Raphson load flow method implemented in ETAP. Newton Raphson method has the advantage of simplicity, accuracy and ease of convergence compared to other methods of load flow.

2.1.2 Voltage stability

One of the greatest attributes of a power system is stability (Penchalaiah, G and Ramya, R, 2022). Power system is said to be stable, when it regains its operating condition after being subjected to disturbances. It can be classified into rotor angle stability, frequency stability and voltage stability. Among these, voltage stability is the most critical as it determined

the balance between reactive power supply and consumption. Voltage stability is the ability of power systems to maintain bus voltages within the acceptable operational limits of $\pm 5\%$ of its nominal value after being subjected to disturbance and in normal operation (Tebeje Thesfaw Wondie and Teshome Goa Tella, 2022). There are many causes of voltage instability in power system. It is caused by sudden increase in the load, long weakly connected transmission lines, or low generation capacity but the main cause of voltage instability is the lack of the power system to supply reactive power (Peter .O. Ohiero and Ekpo O. A, 2022). Voltage instability could be mitigated by employing reactive power compensating devices such as shunt capacitors, SVC, and under load tap changing (ULTC) transformer but it requires proper identification of weak buses or points of connection. Voltage stability is mainly classified as large-disturbance and small-disturbance voltage stability (Xuan Zhang, Hao Yang, etal, 2023). Figure 1 shows the power system consisting of the single generator, transmission line and a load, which is normally Single Machine Infinite Bus System (SMIB).

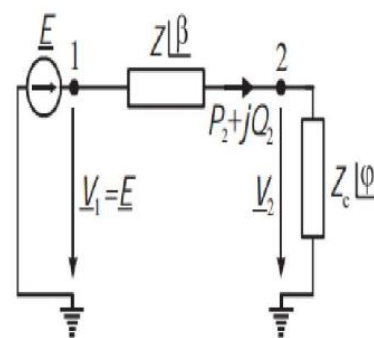


Figure 1: Single Machine Infinite Bus representation of the power system (Sabo, A. etal., 2021)

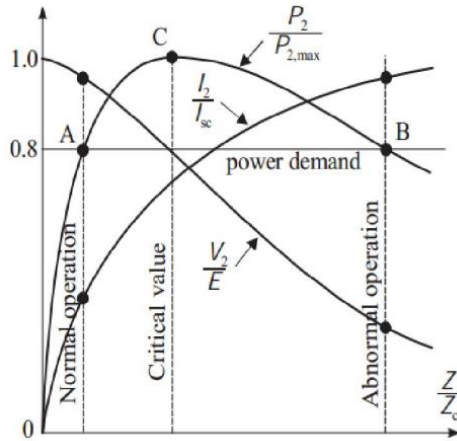


Figure 2: Current, Voltage and Power relation at the load

Figure 2 shows the plot relating received real power (P_2) and reactive power (Q_2), and voltage across the load (V_2).

The current, voltage, power and maximum power at the load terminal are given by the following equations:

$$I = \frac{E}{Z\sqrt{1+2(\frac{Z_c}{Z})\cos(\beta-\varphi)+(\frac{Z_c}{Z})^2}} \quad (1)$$

$$V_2 = |IZ_c| = \frac{EZ_c}{Z\sqrt{1+2(\frac{Z_c}{Z})\cos(\beta-\varphi)+(\frac{Z_c}{Z})^2}} \quad (2)$$

$$P_2 = V_2 I \cos\varphi = \frac{E^2 Z_c}{Z^2\sqrt{1+2(\frac{Z_c}{Z})\cos(\beta-\varphi)+(\frac{Z_c}{Z})^2}} \quad (3)$$

$$P_{2max} = \frac{V_1^2 \cos\varphi}{2Z[1+\cos(\beta-\varphi)]} = \frac{V_1^2 \cos\varphi}{4Z \cos^2[(\beta-\varphi)/2]} \quad (4)$$

If $Z_c = \infty$, $V_1 = V_2$ and there is no current flowing through the circuit but as Z_c decreases, P_2 increases rapidly and slow down as it approaches the maximum value of P_{2max} . On the other hand I approaches the maximum value which is the short circuit current I_{sc} while V_2 decreases exponentially. For a given value of P_2 there exist two operating points on either side of

P_{2max} . The left side operating zone corresponds to the high voltage and low current and is considered a stable operating zone while the right side corresponds to the high current and low voltage, which is considered to be unstable zone.

Assuming the reactance X of the transmission line is far greater than the resistance, R ($X \gg R$), the voltage V_2 can be written as

$$\bar{V}_2 = \bar{E} + jX\bar{I} \quad (5)$$

Such that the complex power S absorbed by the load is given as

$$S = P_2 + jQ_2 = \bar{V}_2 \bar{I}^* = V_2 \left(\frac{\bar{E}_2^* - \bar{V}_2^*}{-jX} \right) \quad (6)$$

$$= \frac{j}{X} (EV_2 \cos(\varphi) + jEV_2 \sin(\varphi) - V_2^2) \quad (7)$$

From equation 6,

$$P_2 = \frac{EV_2}{X} \sin(\varphi) \quad (8)$$

$$Q_2 = \frac{V_2^2}{X} + \frac{EV_2}{X} \cos(\varphi) \quad (9)$$

Equations (8) and (9) give the power flow equations of the lossless transmission network and gives a good approximation for the real network as $R \gg X$ for the transmission cables.

Eliminating φ from (8) and (9) gives

$$V_2^4 + (2Q_2 X - E^2)V_2^2 + X^2(P_2^2 + Q_2^2) = 0 \quad (10)$$

Solving equation (10) for V_2 shows how reactive power and active power relates to voltage stability at the terminal connected to the load. Plotting the graph of $V_2, P_2, \text{ and } Q_2$ in a V, P, Q , can be used to

determine the maximum permissible complex power transferred between the generator and load without losing stability and the maximum real and reactive power that can be sustain by the power system without losing voltage stability.

2.2 Solar power system

Solar power plants utilises the energy of sunlight to generate electricity. There two methods of generating electricity from solar namely, the photovoltaic (PV) and concentrated solar system (M. Shahabuddin, et al., 2021). Among the two, the PV is widely used because of its simplicity, low maintenance and high reliability.

A photovoltaic (PV) system consists of one or more solar panels, inverter(s), storage devices (batteries), charge controllers and other electrical and mechanical devices used to convert energy from the sun to generate electricity. A solar panel consists of numbers photocells that are connected in series and parallel used to generate electricity from solar energy. It is represented by an equivalent circuit shown in Figure 3 which consists of a single diode with a current source, series and parallel resistors. The current source represent the conversion of light to current, while the diode represent the P-N junction which the PV generator is built from and the series and parallel resistors that represent the resistive loses. Generally, the output of a PV array depends on solar radiation, irradiation intensity, ambient temperature, open and short circuit faults and shading influenced the power produced from solar module or panel.

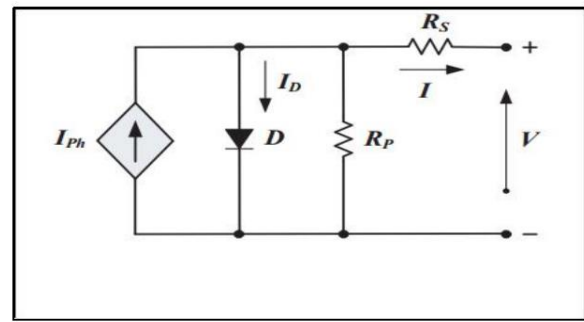


Figure 3: PV cell generator equivalent circuit

When the semiconductor P-N junction is exposed to light, it absorbs the light's energy and transfers it to negatively charged particles in the material called electrons. This extra energy allows the electrons to flow through the material as electrical current. The electrical current flowing to the load from the solar cell is given by;

$$I = I_{ph} - I_s \left[\exp \frac{q(V + IR_s)}{NKT} - 1 \right] - \frac{(V + IR_s)}{R_p} \quad (11)$$

The photocurrent I_{ph} plays a major role on the behaviour of solar module. It depends of the solar irradiance and the temperature and is given by

$$I_{ph} = \left[I_{sc} + K_i(T - T_{ref}) \right] \frac{B}{1000} \quad (12)$$

Another important aspect of solar module is the diode saturation current. This also varies with temperature and can be modelled using

$$I_s(T) = I_{rs} \left(\frac{T}{T_{ref}} \right)^{\frac{3}{N}} e^{-\frac{qV_i}{NK \left(\frac{1}{T} - \frac{1}{T_{ref}} \right)}} \quad (13)$$

The reverse saturation current I_{rs} and the thermal voltage are given in equation (14) and equation (15) respectively.

$$I_{rs} = \frac{I_{sc}}{e^{\frac{qV_{oc}}{NKT}}} \quad (14)$$

$$v_t = \frac{KT}{q} \quad (15)$$

$$V_{oc} = V_{ocs}(1 + \beta_T(T_C - T_R))v_T \quad (16)$$

Once the instantaneous value of V_{ocs} and the photocurrent I_{ph} are known, the voltage and the power of the solar module or array can be obtained.

Where,

I_{rs} is the reverse saturation current (A), v_t is the thermal voltage (V), V_{ocs} is the open circuit voltage at STC, β_T is the temperature correction factor, v_T is the voltage correction factor, β_T and v_T determined empirically, I is the current output to the load (A), V is the terminal voltage/output of the cell (V), I_{ph} is the current of the photovoltaic solar cell (A), I_{sc} is the short circuit current (A), I_s is the diode saturation current (A), N is the ideality factor of the solar cell [/], R_s is the series intrinsic resistance (Ω), R_p is the parallel intrinsic resistance (Ω), K is Boltzmann Constant ($1.380658e^{-23}$ J/K), K_i is the temperature coefficient of the short circuit current, T is the Solar Cell operation Temperature (K), T_{ref} is the temperature reference (K), q is Electron Charge ($1.6022e^{-19}$ Cb), B is solar irradiation in W/m^2 .

2.3 Wind power system

Wind power generator utilises wind kinetic energy to rotate the blades of wind turbine which is converted to mechanical energy

which drives the rotor of the generator coupled to it. The generator further converts the mechanical energy of the rotor to electrical energy, which is either used as standalone or fed into the power grid. The process of converting wind energy into electrical energy is shown in Figure 4. It consists of the rotor blades, the mechanical drive train, the generator, the grid connection interface (power electronic converter) and the electrical grid or network (Nizamani, Z, et al. 2024). Different configurations are used in wind energy conversion system. There are basically two types of wind turbines classification; fixed and variable speed. This is further expanded to fixed speed with squirrel cage induction generator (SCIG), variable speed wind turbine with doubly fed induction generator (DFIG), variable speed permanent magnet synchronous generator (PMSG) and variable speed squirrel induction generator (VSCIG). The choice and optimal selection of generators for wind turbines is based on the characteristics and performance of the generator. Other factors to consider are cost, maintenance, efficiency, reliability and the ability to meet some important grid requirements. A fixed speed squirrel cage induction generator consumes reactive power and cannot contribute to voltage control although compensation capacitor can further improve reactive power compensation and maintain a smooth grid connection. In the absence of a reactive power compensator, voltage fluctuation increases leads and to line losses, reduction in efficiency and performance of the system. However, with the addition of a power converter, squirrel cage induction generator can operate in variable speed.

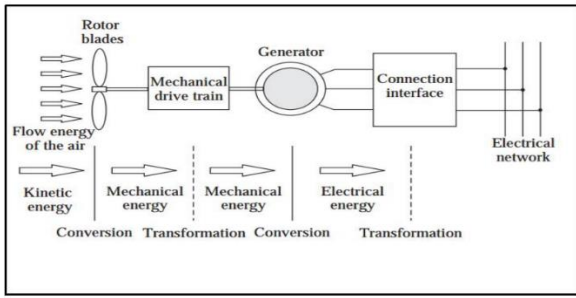


Figure 4: Wind Energy Conversion system

The mechanical power captured by the rotor blades of the wind turbine depends on the velocity of the blowing air passing through the perpendicular area A , swept by the rotor blades and the air density as and is given by equation (17). From equation (17) and (18), it is clear that the power captured by the rotor blades is proportional to the cube power of the wind speed.

$$P_w = \frac{1}{2} \rho A V_w^3 \quad (17)$$

$$P_w = C_p(\lambda, \beta) \frac{1}{2} \rho A V_w^3 \quad (18)$$

The tip speed is given by

$$\lambda = \frac{\omega_r R}{V_w} \quad (19)$$

Where,

P_w is the power of the wind turbine (W),
 C_p is the performance coefficient, λ is the tip speed ratio[/], β is the blade pitch angle, ρ is the air density(1.225kg/m³), 15⁰C at sea level, A is the swept area of the turbine blades ($A = \pi R^2$ (m²))
 R is the rotor radius(m), V_w is the wind speed (m/s²).

Performance coefficient is a function of the tip speed ratio and the blade pitch angle and its maximum value is given as (Castillo, O. C et al., 2023);

$$C_p = C_1 \times (C_2 \times \frac{1}{\lambda_i} - C_3 \times \beta - C_4) \times \exp(-\frac{C_5}{\lambda_i}) + C_6 \times \lambda \quad (20)$$

$$\text{Where, } \left(\frac{1}{\lambda_i} = \frac{1}{\lambda + 0.08 \times \beta} - \frac{0.035}{\beta^3 + 1} \right) \quad (21)$$

In the power characteristics of wind generator, there is a specific point for each wind speed where the output power is maximized. Maximum aerodynamic efficiency is obtained at this specific point on the wind turbine characteristics. At this point, the tip speed ratio of wind turbine must be maintained constant in order to maximise aerodynamic efficiency. It requires running the turbine at optimum C_p to extracted maximum wind power. As wind speed V_w changes, the rotor speed ω_r , changes, therefore, it is necessary to maintain optimum speed ratio. Therefore, the control strategy should be made to follow this trend.

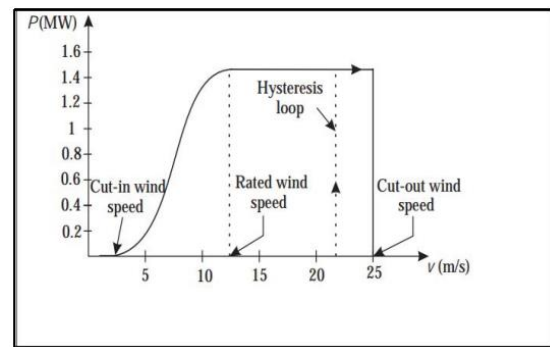


Figure 5: Relationship between the output power of wind turbine and wind speed.

There are three main regions in the wind speed namely the cut-in, rated and cut-out wind speed. The cut-in wind speed is the wind speed the turbine blade start to rotate but is not sufficient to generate power. As the wind speed increase above cut-in wind speed, the turbine begins to generate power. The turbine speed then increases sharply to rated speed where rated power is generated

and remains constant as the wind speed increases. This continue until cut-out speed when the power generated is shot down to protect the wind turbine from damage.

Several wind turbine generators are connected together to form a wind farm or plant to produce the required power. The total or rated power is the summation of the individual wind turbine powers.

2.3.1 Wind turbine generator modelling

In modelling wind turbine generator, models of the basic components of the wind turbine generator such as wind speed model, turbine rotor model, drive-train model, generator model and electrical network model can be carried out as shown in Figure 6.

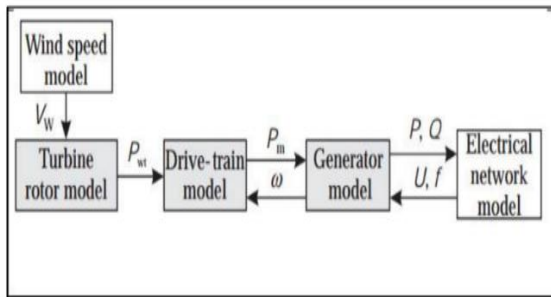


Figure 6: Block diagram for the wind turbine model

Wind speed model requires selection of site or location. Wind speed can be represented based on the historical measurement of wind speed for the proposed wind plant site or modelled analytically. Analytical modelling of wind speed can be achieved using equation (22).

$$V_w(t) = V_{wa}(t) + V_{wr}(t) + V_{wg}(t) + V_{wt}(t) \quad (22)$$

Where,

$V_w(t)$ is the wind speed at a particular time, $V_{wa}(t)$ is the average wind speed, $V_{wr}(t)$ is the ramp component of wind

speed, $V_{wg}(t)$ is the gust component of wind speed, $V_{wt}(t)$ is the turbulence component of wind speed.

The wind turbine is model using equations (18) to equation (21) while the drive-train is model based on a multi mass system represented by the angular position, angular velocity and the inertia of the rotating bodies. The mass objects are connected to each other through the damping coefficient and some spring constants as represented by the two mass system in Figure 7. The two -mass model of wind turbine is given as;

$$2H_t \frac{d\omega_t}{dt} = C_t - K_s(\theta_t - \theta_g) - D_{tg}(\omega_t - \omega_g) \quad (23)$$

$$2H_g \frac{d\omega_g}{dt} = -C_e + K_s(\theta_t - \theta_g) + D_{tg}(\omega_t - \omega_g) \quad (24)$$

$$\frac{d\theta_t}{dt} = \omega_t \quad (25)$$

$$\frac{d\theta_g}{dt} = \omega_g \quad (26)$$

It is the inertia for the rotating blades due to pitch and the drive train (hub, low speed shaft, and rotating parts of the gearbox connected to low-speed shaft), J_g is the inertia for the generator rotor, high-speed shaft and the gearbox parts connected to high-speed shaft.

ω_t is the angular velocity for the turbine, ω_g is the generator angular velocity, θ_t is the turbine rotor, θ_g is the generator rotor, θ_g is the generator rotor, D_{tg} is the mutual damping, K_s is the Shaft stiffness, D_t is the self-damping for the aerodynamic of the turbine blades, D_g is the self-damping for the generator

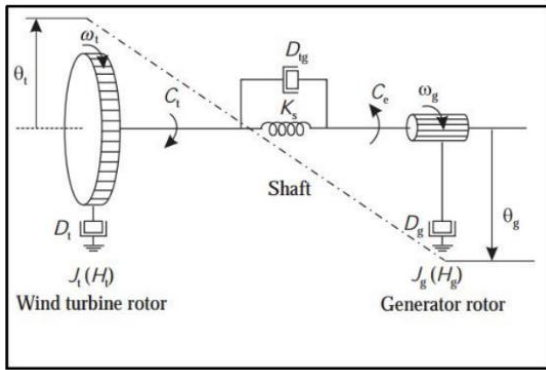


Figure 7: Two-Mass Drive Train

Assuming the velocities of the generator rotor and turbine speed to be equal, the two mass equations of motion can be expressed in reduced form as;

$$2(H_t + H_g) \frac{d\omega_m}{dt} = C_t + C_e \quad (27)$$

2.3.2 Power conditioning system

Both wind and solar power plants need power conditioning system to integrate the generated power to the grid because of their variability and intermittency. Most grids likewise the Nigeria grid operate on Alternating Current AC and solar power plant or PV array produces DC voltage. This requires additional devices to synchronise the PV power with the power grid. Therefore a power conditioning unit is necessary to convert the generated and variable DC power by the solar plant and the variable power from the wind power plant to usable AC power. The power conditioning system consists of power electronic converters such as DC–DC converter, DC – AC inverter, rectifier, and AC–AC converter or transformer and controllers (Siwakoti, Y. P, et al., 2018). DC – DC is used to step up the low magnitude of DC voltage to higher voltage (boost type). Different topologies of power conditioning unit exist (Harbi, I., Rodriguez et al., 2023, Zhang, Z., & Chen, R. (2023) .

The topology can be one stage, two stage or multi stage. In integrating solar and wind power plant to grid, the topologies require more than one conversion stage. For the solar power conversion system, its topology consists of DC-DC converter and DC to AC inverter while the wind power conversion system requires rectifiers to convert the variable frequency AC into DC and a DC/AC inverter to convert DC to AC.

3.0 Methodology

The method used in this study is a computer based software modelling and simulation of load flow of the Nigeria 330kV power network using Newton Raphson method (Mohsin, M. Y et al., 2022) in Electrical Transient Analyzer Program (ETAP) software. Electrical Transient Analyzer Program is an electrical network modelling and simulation software tool used by power systems engineers to create an electrical power system model and analyse electrical power system dynamics, transients and protection. The model of the complete network requires data of components such as the real and reactive power of the generators, the real and reactive power of the transformers and loads, the transmission lines parameters and length as well as the number of line circuit (single or double) and the size and types of cable and configuration. All these data were obtained from the Transmission Company of Nigeria, Calabar. The data for the solar power generator and wind power generator were also obtained as shown in table A3 and A4 in the appendix.

3.1 Description of the Nigerian 330kV transmission network

The transmission of bulk power in Nigeria is at a voltage of 132kV and 330kV and this is handled by the Transmission Company of Nigeria (TCN). Figure 8 shows a single line

diagram of the Nigerian 330kV network. It has a theoretical wheeling capacity of 7,000MW but in practice the wheeling capacity is 4,000MW. Due to the inadequate power supply the Federal Government of Nigeria in 2012 awarded a contract for a grid connected wind farm of 10MW at Katsina State and 10MW of solar farm at Rimi in Kano State. These projects are yet to be completed and integrated into the grid. Before integration, it is necessary to study the effect it will have on the stability of the grid and how subsequent expansion or penetration level will affect the grid stability. The study is concerned with the voltage stability, power losses and maximum level of penetration beyond which the stability especially voltage stability limit of the network will be violated and the power losses. The parameters of the network components are as attached in Appendix 1.

3.1.1 The Katsina 10MW wind farm in Nigeria

The Katsina Wind Farm is a 10MW wind farm located in a small village called Rimi which is 25km away from the Katsina city in Northern Nigeria. It consists of 37 GEV MP 275-kW wind turbine generator. It will be the first wind farm and carried out by VERGNET and the FEDERAL MINISTRY OF POWER (FMP). The Federal Ministry of Energy of Nigeria has selected the company VERGNET for the robustness of its machines and their easy installation and maintenance that need less important logistics than traditional wind turbines. Part of the responsibilities of VERGNET is to train technicians to help the FMP as part of maintenance. This partnership could lead to the construction of wind farms in other states of Nigeria and increase the penetration level of wind

generators into the grid. The Technical characteristics are as follows; WTG number: 37 GEV MP, Rated power: 275 kW, Total power: 10.175 MW, Rotor diameter: 32 m, Tower height: 55 m, Swept area 804.25m², Number of blades 2, Cut in wind speed 3.5 m/s, Cut out wind speed 25 m/s, Tower type: Tubular.

3.1.2 Kano 10 MW solar power plant in Nigeria

The Kano 10MW solar power plant is presently the largest grid connected solar farm in Nigeria. It is a ground mounted solar plant occupying over 24 hectares of land. It involves the installation and operation of a 10 MW solar power plant in the Challawa Industrial Area in Kumbotso Local Government Area of Kano State, as a demonstration pilot project to stimulate investment in the Nigerian power sector. The solar plant comprises over 21,000 solar PV panels, two 6MVA transformers, 52 inverters, and a 12km evacuation infrastructure.

3.2 System modelling and configuration

Figure 9 shows the ETAP model of the Nigeria 330kV transmission network. The data collected about each of the components such as generators (thermal, hydro, etc.), transformers, transmission lines and load were inputted into their respective model in ETAP software. The solar power plant in Kano State is connected to the 330kV transmission network at Kano State while the wind farm at Katsina State is connected to the 132kV substation at Katsina State and integrated into the 330kV network at Kano State. The solar farms generate at a voltage of 16kV which is stepped up to 132kV and then connected to the 330kV Kano substation. The data and parameters of the components

are shown in Table A1, A2, A3 and A4 in the appendix. The solar power plants is modelled based on SUNTECH solar panel

while the wind power plant was modelled based on Doubly Fed Induction Generator (DFIG) driven by wind turbine.

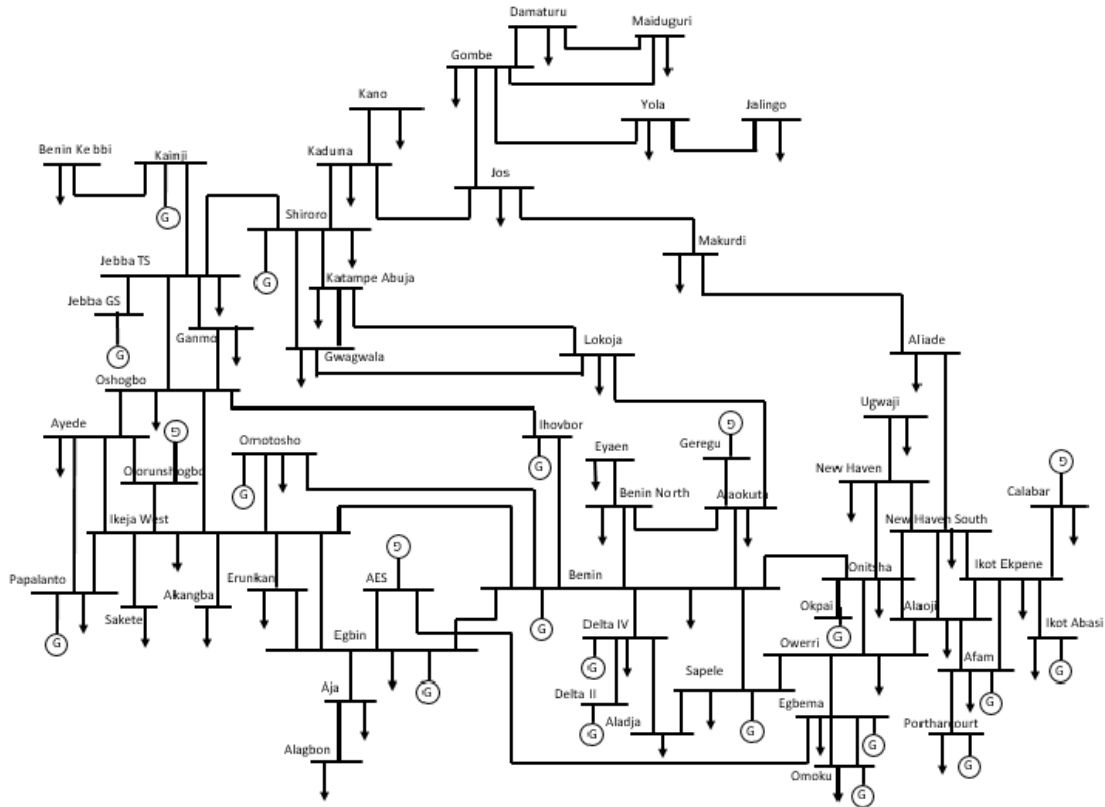


Figure 8: Single line diagram of the 55-bus Nigerian 330kV Transmission Network

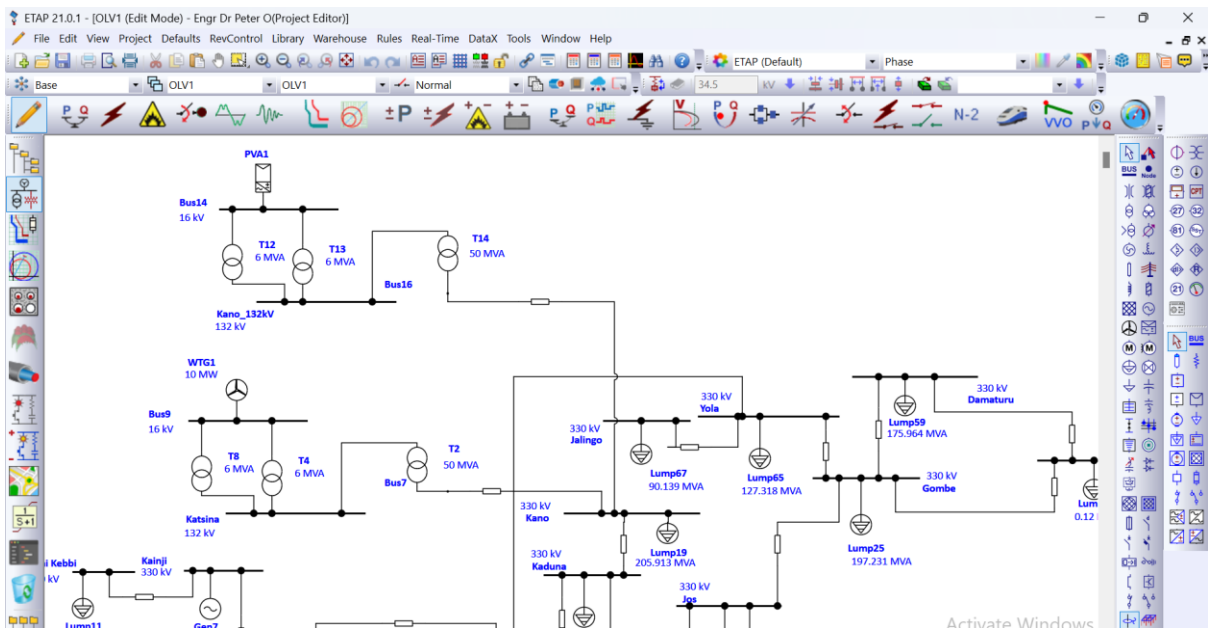


Figure 9: A section of the modelled of the Nigerian 330kV power network

4.0 Results and discussions

4.1 Voltage stability studies

The load flow, voltage stability and power loss simulation studies were carried out in ETAP based on Newton Raphson load flow method. Four scenarios were considered in this paper and in each scenario, the voltage, power flow and power losses were recorded. In (iv), considerations was given to the best combination that will not violate voltage stability or beyond which the stability limits of $\pm 5\%$ of the nominal voltage (0.95pu to 1.05pu).

- i. The existing network only
- ii. Solar PV Generation only
- iii. Wind Generation only and
- iv. Hybrid (Solar and Wind Generation).

4.1.1 The existing network only.

The voltage stability studies were conducted by performing the load flow under the existing network only as shown in Figure 10. For each case, the voltage magnitude and angle were recorded. In addition to the load flow analysis, the weak buses in the network were identified since they results to violation of voltage stability

limit. Table 1 shows the voltage magnitude in kilovolt and per unit (pu) and angles at each bus when no renewable power plant is connected to the grid. From the results weak buses whose voltage falls below the voltage stability limit of $\pm 5\%$ of the nominal voltage of 330kV (1.00pu) were identified to be Aliade 0.9469<-26.18 pu, Damaturu 0.83162<-34.6pu, Gombe 0.86430<-33.1pu, Jalingo 0.86331<-23.3pu, Jos 0.90205<-31.2pu, Kaduna 0.87847<-33.6pu, Kano 0.77426<-43.8pu, Makurdi 0.94202<-26.4pu, Maiduguri 0.86735<-34.2pu, Yola 0.8920<-23.39pu. Among the buses, Kano bus is the weakest with a voltage of 0.77426<-43.8pu followed by Damaturu bus with a voltage of 0.83162<-34.6pu. This voltage violation are mostly dominated in the Northern part of the country due to the consumption of reactive power by the long transmission lines from the generators which are concentrated in the southern part of the country.

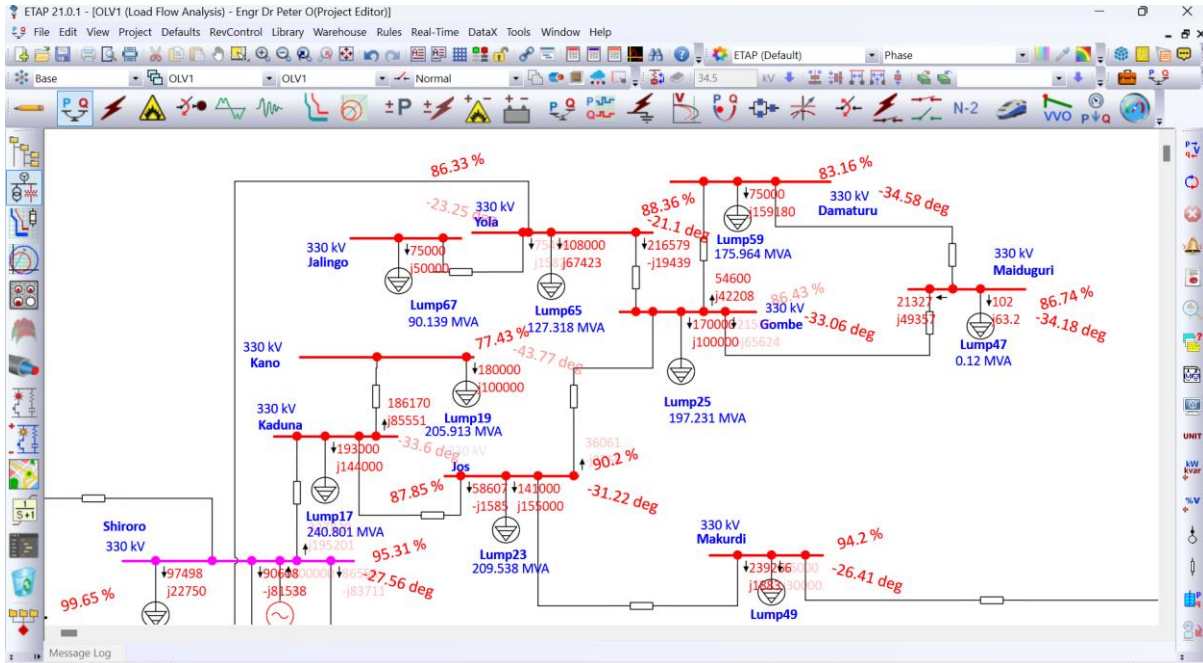


Figure 10: A section of the simulation model of the Nigerian 330kV power network.

Table 1: Simulation results of bus voltages without the integration renewable power plants

S/N	Bus Name	Bus Nominal Voltage (kV)	Operational Voltage (%)	Operational Voltage (kV)	V (pu)	Angle (°)
1.	AES	330	99.301	327.6933	0.99301	-2.8
2.	Afam GS	330	97.094	320.4102	0.97094	-15.1
3.	Ayiede	330	96.957	319.9581	0.96957	-14.7
4.	Aja	330	99.52	328.416	0.9952	-0.458
5.	Ajaokuta	330	96.012	316.8396	0.96012	-27.00
6.	Akamgba	330	95.799	316.1367	0.95799	-12.9
7.	Aladja	330	99.265	327.5745	0.99265	-20.20
8.	Alaoji	330	97.237	320.8821	0.97237	-15.1
9.	Alaogbon	330	99.06	326.898	0.9906	-0.886
10	Aliade	330	94.69	312.477	0.9469	-26.18
11.	B.Kebbi	330	98.51	325.083	0.9851	-23.39
12.	Benin	330	97.73	322.509	0.9773	-19.32
13.	Benin North	330	95.76	316.008	0.9576	-21.68
14.	Calabar	330	96.59	318.747	0.9659	-17.5
15	Damaturu	330	83.162	274.43	0.83162	-34.6
16.	Delta	330	100.0	330	1.0000	-20.26
17.	Egbema	330	97.68	322.344	0.9768	-10.64
18.	Egbin PS	330	100.0	330	1.0000	0

**INVESTIGATING THE EFFECT OF INTEGRATION OF RENEWABLE POWER PLANTS ON THE NIGERIA
330KV ELECTRICITY GRID**

Martin, et al.

19	Erunkan	330	98.08	323.664	0.9808	-5.51
20	Eyaen	330	95.589	323.664	0.9808	-21.5
21	Ganmo	330	95.40	314.82	0.954	-20.75
22	Geregu	330	96.01	316.833	0.9601	-27.5
23	Gombe	330	86.430	285.219	0.86430	-33.1
24	Gwagwalada	330	95.84	316.272	0.9584	-29.11
25	Ihovbor	330	96.61	318.813	0.9661	-19.14
26	Ikeja West	330	97.04	320.232	0.9704	-11.48
27	Ikot Abasi	330	96.55	318.615	0.9655	-17.39
28	Ikot Ekpene	330	96.64	318.912	0.9664	-17.38
29	Jalingo	330	86.332	284.8956	0.86332	23.3
30	Jebba GS	330	100	330	1.0000	-18.5
31	Jebba TS	330	99.65	328.845	0.9965	-18.79
32	Jos	330	90.205	297.6765	0.90205	-31.2
33	Kainji	330	100.9	332.97	1.0090	-17.25
34	Kaduna	330	87.847	289.8951	0.87847	-33.6
35	Kano	330	77.426	255.5058	0.77426	-43.8
36	Katampe (Abuja)	330	95.75	315.975	0.9575	-29.28
37	Lokoja	330	95.95	316.635	0.9595	-28.38
38	Makurdi	330	94.202	310.8666	0.94202	-26.4
39	Maiduguri	330	86.735	286.2255	0.86735	-34.2
40	New Haven	330	97.0	320.1	0.9700	-20.13
41	New Haven South	330	97.01	320.133	0.9701	-20.09
42	Olorunshogo	330	101.8	335.94	1.018	-10.37
43	Omosho	330	100.0	330	1.0000	-16.50
44	Omoku	330	97.79	322.707	0.9779	-10.64
45	Oshogbo	330	97.41	321.453	0.9741	-18.92
46	Okpai	330	98.61	325.413	0.9861	-17.84
47	Onitsha	330	98.23	324.159	0.9823	-17.81
48	Owerri	330	97.6	322.08	0.976	-13.45
49	Papalanto	330	97.09	320.397	0.9709	-12.97
50	PortHarcourt	330	95.69	315.777	0.9569	-16.69
51	Sapele	330	98.31	324.423	0.9831	-19.04
52	Sakete	330	95.22	314.226	0.9522	-13.31
53	Shiroro	330	95.51	315.183	0.9551	-28.22
54	Ugwuaji	330	96.89	319.737	0.9689	-20.21
55	Yola	330	89.20	294.36	0.892	-23.39

INVESTIGATING THE EFFECT OF INTEGRATION OF RENEWABLE POWER PLANTS ON THE NIGERIA
330KV ELECTRICITY GRID

Martin, et al.

9.	Alaogbon	330	99.062	326.9046	0.99062	-0.9
10.	Aliade	330	95.265	314.3745	0.95265	-25.0
11.	B.Kebbi	330	98.521	325.1193	0.98521	-23.0
12.	Benin	330	97.846	322.8918	0.97846	-19.00
13.	Benin North	330	95.895	316.4535	0.95895	-21.68
14.	Calabar	330	97.060	320.298	0.97060	-17.0
15.	Damaturu	330	84.598	279.1734	0.84598	-34.3
16.	Delta	330	100.0	330	1.0000	-19.9
17.	Egbema	330	98.059	323.5947	0.98059	-10.3
18.	Egbin PS	330	100.0	330	1.0000	0
19.	Erunkan	330	98.125	323.8125	0.98125	-5.4
20.	Eyaen	330	95.697	315.8001	0.95697	-21.5
21.	Ganmo	330	95.449	314.9817	0.95449	-20.4
22.	Geregu	330	96.405	318.1365	0.96405	-26.9
23.	Gombe	330	87.713	289.4529	0.87713	-32.8
24.	Gwagwalada	330	96.189	317.4237	0.96189	-28.4
25.	Ihovbor	330	97.719	322.4727	0.97719	-18.8
26.	Ikeja West	330	97.117	320.4861	0.97117	-11.3
27.	Ikot Abasi	330	97.109	320.4597	0.97109	-16.7
28.	Ikot Ekpene	330	97.601	322.0833	0.97601	-16.3
29.	Jalingo	330	87.167	287.6511	0.87167	23.2
30.	Jebba GS	330	100	330	1.0000	-18.1
31.	Jebba TS	330	99.665	328.8945	0.99665	-18.40
32.	Jos	330	91.133	300.7389	0.91133	-31.1
33.	Kainji	330	100.941	333.1053	1.00941	-16.9
34.	Kaduna	330	88.762	292.9146	0.88762	-33.4
35.	Kano	330	78.909	260.3997	0.78909	-43.3
36.	Katampe (Abuja)	330	96.093	317.1069	0.96093	-28.6
37.	Lokoja	330	96.273	317.700.9	0.96273	-27.8
38.	Makurdi	330	94.872	313.0776	0.94872	-26.3
39.	Maiduguri	330	88.149	290.8917	0.88149	-33.9
40.	New Haven	330	97.508	321.7764	0.97508	-19.4
41.	New Haven South	330	97.523	321.8259	0.97523	-19.4
42.	Olorunshogo	330	101.906	336.2898	1.01906	-10.2
43.	Omosho	330	100.0	330	1.0000	-16.2
44.	Omoku	330	98.112	323.7696	0.99112	-10.3
45.	Oshogbo	330	97.484	321.6972	0.97484	-18.6

Table 3: Simulation results of bus voltages with the integration of 10MW wind power plants

S/N	Bus Name	Bus Nominal Voltage (kV)	Operational Voltage (%)	Operational Voltage (kV)	V (pu)	Angle ($^{\circ}$)
1.	AES	330	100	330	1	-2.9
2.	Afam GS	330	100.422	331.3926	1.00422	-15.1
3.	Ayiede	330	96.989	320.0637	0.96989	-14.7
4.	Aja	330	99.518	328.4094	0.99518	-0.5
5.	Ajaokuta	330	100.654	332.1582	1.00654	-26.2
6.	Akamgba	330	96.087	317.0871	0.96087	-12.7
7.	Aladja	330	99.576	328.6008	0.99576	-19.8
8.	Alaoji	330	97.470	321.651	0.9747	-15.1
9.	Alaogbon	330	99.062	326.9046	0.99062	-0.9
10.	Aliade	330	95.102	313.8366	0.95102	-24.9
11.	B.Kebbi	330	98.517	325.1061	0.98517	-22.9
12.	Benin	330	97.380	321.354	0.9738	-18.9
13.	Benin North	330	95.868	316.3644	0.95868	-21.2
14.	Calabar	330	96.999	320.0967	0.96999	-16.9
15.	Damaturu	330	84.213	277.9029	0.84213	-34.3
16.	Delta	330	100.0	330	1	-19.8
17.	Egbema	330	98.033	323.5089	0.98033	-10.3
18.	Egbin PS	330	100.0	330	1	0
19.	Erunkan	330	98.130	323.829	0.9813	-5.4
20.	Eyaen	330	95.670	315.711	0.9567	-21.4
21.	Ganmo	330	95.444	314.9652	0.95444	-20.3
22.	Geregu	330	96.253	317.6349	0.96253	-26.8
23.	Gombe	330	87.369	288.3177	0.87369	-32.8
24.	Gwagwalada	330	95.979	316.7307	0.95979	-28.1
25.	Ihovbor	330	97.709	322.4397	0.97709	-18.7
26.	Ikeja West	330	97.123	320.5059	0.97123	-11.3
27.	Ikot Abasi	330	97.049	320.2617	0.97049	-16.8
28.	Ikot Ekpene	330	97.541	321.8853	0.97541	-16.2
29.	Jalingo	330	86.982	287.0406	0.86982	23.1
30.	Jebba GS	330	100	330	1	-18.1
31.	Jebba TS	330	99.661	328.8813	0.99661	-18.30
32.	Jos	330	90.824	299.7192	0.90824	-30.9
33.	Kainji	330	100.938	333.0954	1.00938	-16.8

34.	Kaduna	330	88.304	291.4032	0.88304	-33.1
35.	Kano	330	77.674	256.3242	0.77674	-42.6
36.	Katampe (Abuja)	330	95.886	316.4238	0.95886	-28.4
37.	Lokoja	330	96.096	317.1168	0.96096	-27.6
38.	Makurdi	330	94.683	312.4539	0.94683	-26.2
39.	Maiduguri	330	87.770	289.641	0.8777	-33.9
40.	New Haven	330	97.426	321.5058	0.97426	-19.4
41.	New Haven South	330	97.441	321.5553	0.97441	-19.3
42.	Olorunshogo	330	101.912	336.3096	1.01912	-10.2
43.	Omosho	330	100.0	330	1	-16.1
44.	Omoku	330	98.086	323.6838	0.98086	-10.3
45.	Oshogbo	330	97.479	321.6807	0.97479	-18.5
46.	Okpai	330	98.965	326.5845	0.98965	-17.3
47.	Onitsha	330	98.581	325.3173	0.98581	-17.2
48.	Owerri	330	97.930	323.169	0.9793	-13.0
49.	Papalanto	330	97.176	320.6808	0.97176	-12.8
50.	PortHarcourt	330	96.094	317.1102	0.96094	-16.1
51.	Sapele	330	98.412	324.7596	0.98412	-18.6
52.	Sakete	330	95.310	314.523	0.9531	-13.1
53.	Shiroro	330	95.627	315.5691	0.95627	-27.3
54.	Ugwuaji	330	97.315	321.1395	0.97315	-19.50
55.	Yola	330	88.986	293.6538	0.88986	-21.0

4.2 Voltage stability with the integration of both solar and wind power plants

In the fourth case, both the 10MW Solar Power plant and the 10MW wind power plant was integrated to the existing grid as shown in Figure 13. The results of voltage magnitude and angles obtained from the load flow simulation when both solar and wind power were connected to the electricity grid is shown in Table 4. From the results it can be seen that there is increase in the voltage magnitude when both solar and wind power plant were connected to the grid. The voltage magnitude of all the buses improved, for

example the voltage magnitude of Jalingo bus improved from $0.86332 \angle -23.3^\circ$ pu to $0.93380 \angle -22.45^\circ$ pu a difference 0.07048 pu Figure 14 shows the comparison between the four scenarios. While there is little increase in the voltage magnitude when either solar or wind power plant is connected to the grid, there is a reasonable increase when both 10MW solar power plant and 10MW wind power plant were integrated into the grid which resulted to improvement of an average 3.3% increase in the voltage magnitude of the buses in the network.

INVESTIGATING THE EFFECT OF INTEGRATION OF RENEWABLE POWER PLANTS ON THE NIGERIA 330KV ELECTRICITY GRID

Martin, et al.

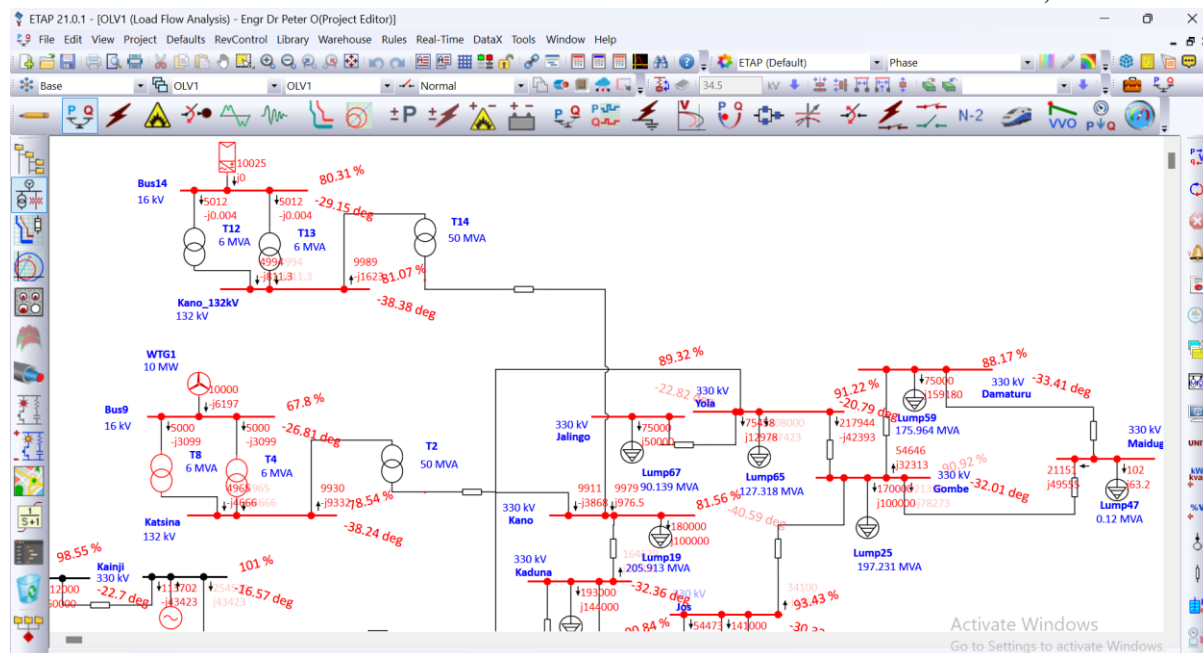


Figure 13: A section a model of the network when both the 10MW solar power plant and 10MW wind power plants were connected to the grid.

Table 4: Simulation results of bus voltages with the integration of both 10MW solar power plant and the 10MW wind power plants

S/N	Bus Name	Bus Nominal Voltage (kV)	Operational Voltage (%)	Operational Voltage (kV)	V (pu)	Angle (°)
1.	AES	330	100.759	332.505	1.00759	-2.9
2.	Afam GS	330	100.300	330.9903	1.00300	-14.9
3.	Ayiede	330	98.153	323.9052	0.98153	-14.5
4.	Aja	330	100.427	331.4094	1.00427	-0.5
5.	Ajaokuta	330	100.010	330.0333	1.00010	-26.1
6.	Akamgba	330	96.932	319.8759	0.96932	-12.7
7.	Aladja	330	100.391	331.2906	1.00391	-19.7
8.	Alaoji	330	100.396	331.3071	1.00396	-14.9
9.	Alaogbon	330	99.971	329.9046	0.99971	-0.9
10.	Aliade	330	100.195	330.6438	1.00195	-24.3
11.	B.Kebbi	330	99.518	328.4097	0.99518	-22.5
12.	Benin	330	99.303	327.7002	0.99303	-18.6
13.	Benin North	330	97.566	321.9681	0.97566	-20.9
14.	Calabar	330	100.080	330.2643	1.00080	-16.7
15.	Damaturu	330	94.407	311.5434	0.94407	-32.4
16.	Delta	330	100.909	333	1.00909	-19.5
17.	Egbema	330	100.193	330.6372	1.00193	-10.2
18.	Egbin PS	330	100.909	333	1.00909	0

19.	Erunkan	330	99.141	327.1656	0.99141	-5.4
20.	Eyaen	330	97.368	321.3147	0.97368	-21.1
21.	Ganmo	330	96.553	318.6252	0.96553	-19.9
22.	Geregu	330	100.012	330.0399	1.00012	-26.1
23.	Gombe	330	96.645	318.9288	0.96645	-31.1
24.	Gwagwalada	330	100.516	331.7031	1.00516	-27.4
25.	Ihovbor	330	99.059	326.895	0.99059	-18.4
26.	Ikeja West	330	98.223	324.1362	0.98223	-11.2
27.	Ikot Abasi	330	100.103	330.3402	1.00103	-16.1
28.	Ikot Ekpene	330	100.596	331.9671	1.00596	-16.1
29.	Jalingo	330	93.343	308.0322	0.93343	22.5
30.	Jebba GS	330	100.909	333	1.00909	-17.6
31.	Jebba TS	330	100.647	332.1354	1.00647	-17.9
32.	Jos	330	98.104	323.7435	0.98104	-29.7
33.	Kainji	330	101.925	336.3528	1.01925	-16.4
34.	Kaduna	330	95.790	316.1073	0.95790	-31.5
35.	Kano	330	89.442	295.1589	0.89442	-38.4
36.	Katampe (Abuja)	330	100.384	331.2675	1.00384	-27.6
37.	Lokoja	330	100.200	330.6603	1.00200	-26.9
38.	Makurdi	330	100.221	330.7296	1.00221	-25.5
39.	Maiduguri	330	97.842	322.8789	0.97842	-32.1
40.	New Haven	330	100.946	333.1221	1.00946	-19.1
41.	New Haven South	330	100.975	333.2178	1.00975	-19.0
42.	Olorunshogo	330	103.050	340.0653	1.03050	-10.0
43.	Omotosho	330	100.909	333	1.00909	-15.8
44.	Omoku	330	100.247	330.8154	1.00247	-10.2
45.	Oshogbo	330	98.705	325.7268	0.98705	-18.2
46.	Okpai	330	101.771	335.8446	1.01771	-17.1
47.	Onitsha	330	101.380	334.5543	1.01380	-17.0
48.	Owerri	330	100.358	331.1817	1.00358	-12.9
49.	Papalanto	330	98.304	324.4035	0.98304	-12.6
50.	PortHarcourt	330	99.094	327.0105	0.99094	-16.0
51.	Sapele	330	99.898	329.6637	0.99898	-18.3
52.	Sakete	330	96.415	318.1698	0.96415	-13.0
53.	Shiroro	330	100.546	331.8021	1.00546	-26.3
54.	Ugwuaji	330	100.839	332.769	1.00839	-19.20
55.	Yola	330	95.116	313.8831	0.95116	-20.6

INVESTIGATING THE EFFECT OF INTEGRATION OF RENEWABLE POWER PLANTS ON THE NIGERIA 330KV ELECTRICITY GRID

Martin, et al.

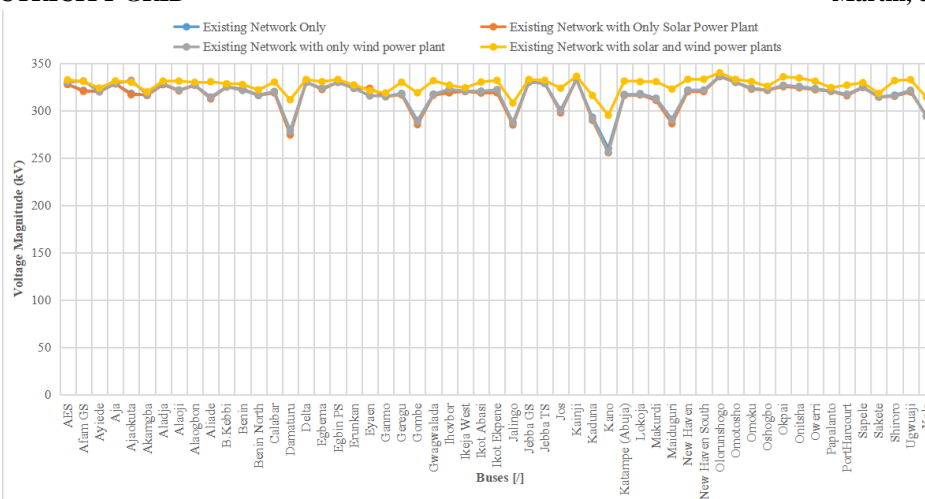


Figure 14 Bus voltages for existing network, solar, wind and hybrid power system.

Table 5: Total power losses

Scenario	Existing network without Renewable integration	Existing network with only 10MW solar plant integration	Existing network with only 10MW wind plant integration	Existing network with both 10MW solar plant and 10MW wind plant integration
Power losses (kW)	256,533.2 (kW)	249, 455.9(kW)	250,319.0 (kW)	246,013.0 (kW)
	-2478, 719.1 (kVAr)	-2611,986.0 (kVAr)	-2443,28.2 (kVAr)	2666,241.5 (kVAr)
Percentage Real power losses Reduction (%)	0	2.76	2.42	4.10

Table 6: Bus voltage and penetration Level of the renewable power plant.

Penetration (MW)	Jos	Kaduna	Kano	Jalingo	Yola	Gombe	Damaturu	Maiduguri
20	0.9852	0.9655	0.9205	0.9338	0.9511	0.9728	0.9520	0.9861
30	0.9865	0.9656	0.9173	0.9355	0.9528	0.9749	0.9543	0.9885
40	0.9873	0.9654	0.9135	0.9369	0.9541	0.9766	0.9562	0.9903
50	0.9879	0.9648	0.9090	0.9381	0.9552	0.9779	0.9575	0.9917

4.3 Power losses

Table 5 shows the power losses in the network when no solar and wind power plant is connected and when there are connected. The results shows that addition of solar and wind power to the grid results in reduction of power losses of the network. In all, the connection of a 10MW solar and 10MW wind power plants results to about 4.10% reduction in power losses.

The level of penetration of solar and wind power plant were increased to know the maximum permissible value that can be integrated at the Kasina 132kV Substation and Kano 330kV substation. This time the focus is on the states within the vicinity of the solar and wind power plants. Table 6 shows the level of perpetration of solar and wind power plants into the grid and the corresponding voltage magnitude. From the results, it can be seen that the voltage level of the buses within the vicinity of the solar and wind power plants increases as the penetration level increases, however, it was observed that the voltage at Kano bus reduces as the penetration level increases. The results shows that the maximum level of penetration that can maintain voltage near stability with the existing network is 20MW beyond which the network will experience voltage stability limit violation.

4.0 Conclusions and recommendations

The study of the effect of integration of solar and wind power plants into the Nigeria 330kV power grid was carried out. The existing Nigeria 330 transmission network was modelled in ETAP and load flow analysis conducted based on Newton Raphson method. Four case scenarios were studied, the existing network only, the solar power plant connected into the existing network, the wind power plant connected into the existing network and the hybrid of

solar and wind power plants. In each of these a steady state load flow was performed to determine the voltage magnitude and angles as well as the maximum penetration level. The voltage magnitude increases as the solar and wind connected to the network. For the level of penetration, while the voltage of other buses increases as the level of penetration increases, the voltage magnitude at the Kano bus decreases. It is recommended therefore that a voltage compensator is required to be connected to Kano buses in order to maintain the bus voltage within the stability limit.

References

- Bukola Babatunde Adetokun, Christopher Maina Muriithi, (2021), Impact of integrating large-scale DFIG-based wind energy conversion system on the voltage stability of weak national grids: A case study of the Nigerian power grid, Energy Reports, Volume 7, 2021, Pages 654-666, ISSN2352-4847, <https://doi.org/10.1016/j.egy.2021.01.025>.
- Castillo, O. C., Andrade, V. R., Rivas, J. J. R., & González, R. O. (2023). Comparison of power coefficients in wind turbines considering the tip speed ratio and blade pitch angle. *Energies*, 16(6), 2774.
- Elemo, E.O., Ogobor, E.A., Alagbe, G.A., Ayantunji, B.G., Mangete, O.E., Tomori, O.S., Doherty, K.B. and Onuh, B.O. (2021) Statistical Analysis of the Average Wind Speeds and Maximum Wind Speed (Gust Winds) at a Location in Abuja, Nigeria. *Open Access*

- Library Journal*, **8**, 1-22. doi: [10.4236/oalib.1107935](https://doi.org/10.4236/oalib.1107935).
- Eissa (SIEEE), M. M. (2015). Protection techniques with renewable resources and smart grids—A survey. *Renewable and Sustainable Energy Reviews*, *52*, 1645–1667. doi:10.1016/j.rser.2015.08.031.
- Harbi, I., Rodriguez, J., Poorfakhraei, A., Vahedi, H., Guse, M., Trabelsi, M., & Kennel, R. (2023). Common DC-link multilevel converters: topologies, control and industrial applications. *IEEE Open Journal of Power Electronics*.
- IRENA (2023)], *Renewable Energy Roadmap: Nigeria*, International Renewable Energy Agency, Abu Dhabi.
- Lawa Salisu and Dr. Isa Garba (2013), *Electricity Generation Using Wind in Katsina State, Nigeria*, International Journal of Engineering Research & Technology (IJERT), Vol. 2 Issue 2, pp 1-13, February - 2013, ISSN: 2278-0181.
- M. Shahabuddin, M.A. Alim, Tanvir Alam, M. Mofijur, S.F. Ahmed, Greg Perkins, A critical review on the development and challenges of concentrated solar power technologies, *Sustainable Energy Technologies and Assessments*, Volume 47, 2021, 101434, ISSN 2213-1388, <https://doi.org/10.1016/j.seta.2021.101434>.
- M. Singh, M. H. V and V. H. S, "Investigation on Power System Stability with Integration of Renewable Resources," *2022 IEEE 10th Power India International Conference (PIICON)*, New Delhi, India, 2022, pp. 1-6, doi: 10.1109/PIICON56320.2022.10045098.
- M. J. Mbunwe and A. O. Ekwue (2020), VOLTAGE STABILITY ANALYSIS OF THE NIGERIAN POWER SYSTEM USING ANNEALING OPTIMIZATION TECHNIQUE, *Nigerian Journal of Technology (NIJOTECH)* Vol. 39, No. 2, April 2020, pp. 562- 571, Print ISSN: 0331-8443, Electronic ISSN:2467-8821, www.nijotech.com, <http://dx.doi.org/10.4314/njt.v39i2.27>.
- Mohsin, M. Y., Khan, M. A. M., Yousif, M., Chaudhary, S. T., Farid, G., & Tahir, W. (2022). Comparison of Newton Raphson and Gauss Seidal Methods for Load Flow Analysis. *International Journal of Electrical Engineering & Emerging Technology*, *5*(1), 01-07.
- Nizamani, Z., Muhammad, A. K., Ali, M. O. A., Wahab, M. A., Nakayama, A., & Ahmed, M. M. (2024). Renewable wind energy resources in offshore low wind speeds regions near the equator: A review. *Ocean Engineering*, *311*, 118834.
- Peter .O. Ohiero and Ekpo O. A, (2022),

- Evaluation of Voltage Stability of Power System Network Considering the Effect of Static var Compensator, *Journal of Science, Engineering and Technology*, Vol. 9 (2), September 2022: pages 63-75.
- Penchalaiah, G., Ramya, R. (2022). Investigation on Power System Stability Improvement Using Facts Controllers. In: Subramani, C., Vijayakumar, K., Dakyo, B., Dash, S.S. (eds) *Proceedings of International Conference on Power Electronics and Renewable Energy Systems. Lecture Notes in Electrical Engineering*, vol 795. Springer, Singapore.
https://doi.org/10.1007/978-981-16-4943-1_46
- Sabo, A., Abdul Wahab, N. I., Othman, M. L., Mohd Jaffar, M. Z. A., Beiranvand, H., & Acikgoz, H. (2021). Application of a neuro-fuzzy controller for single machine infinite bus power system to damp low-frequency oscillations. *Transactions of the Institute of Measurement and Control*, 43(16), 3633-3646.
- Siwakoti, Y. P., Forouzesh, M., & Pham, N. H. (2018). Power electronics converters—An overview. *Control of Power Electronic Converters and Systems*, 3-29.
- Tebeje Tesfaw Wondie, Teshome Goa Tella, (2022), Voltage Stability Assessments and Their Improvement Using Optimal Placed Static Synchronous Compensator (STATCOM), *Journal of Electrical and Computer Engineering*, vol. 2022, Article ID 2071454, 12 pages, 2022.
<https://doi.org/10.1155/2022/2071454>.
- Xuan Zhang, Hao Yang, Guiping Zhou, Yuanzhu Zhao, Dongbo Guo, (2023), Steady-state voltage stability assessment of new energy power systems with multi quadrant power modes, *Energy Reports*, Volume 9, 2023, Pages 3851-3860, ISSN 2352-4847.
- Zhang, Z., & Chen, R. (2023). *Design of Three-phase AC power electronics converters*. John Wiley & Sons.

Appendix

Table A1. Generator and Load Bus Data for the existing Nigerian 330kV, 56-bus power transmission grid						
SN	Bus Name	Bus Nominal Voltage (V)	Generation		Load	
	From		Max. Active Power (MW)	Active Power Schedule (MW)	Active (MW)	Reactive (MVar)
1	AES	330	270	200	-	-
2	Afam GS	330	776	500	-	-
3	Ayiede	330	-	-	270	166.10
4	Aja	330	-	-	220	103
5	Ajaokuta	330	-	-	96	45
6	Akamgba	330	-	-	471	156.071
7	Aladja	330	-	-	167	20
8	Alaoji	330	1079	450	266.18	155
9	Alaogbon	330	-	-	220	103
10	Aliade	330	-	-	136	84
11	B.Kebbi	330	-	-	112	60
12	Benin	330	-	-	298	131.2
13	Benin North	330	-	-	80	50
14	Calabar	330	561	240	110.75	60.37
15	Damaturu	330	-	-	75	259.18
16	Delta I -IV	330	960	620	-	-
17	Egbema	330	378	200	-	-
18	Egbin PS	330	1320	610	-	-
19	Egbin TS	330	-	-	-	-
20	Erunkan	330	-	-	14.5	8.93
21	Ganmo	330	-	-	270	223.35
22	Geregu	330	434	200	-	-
23	Gombe	330	-	-	180	100
24	Gwagwalada	330	-	-	75	65
25	Ihovbor	330	451	182	-	-
26	Ikeja West	330	-	-	510	115
27	Ikot Abasi	330	195	0	-	-
28	Ikot Ekpene	330	-	-	45.8	20
29	Jalingo	330	-	-	75	50
30	Jebba GS	330	590	475	-	-
31	Jebba TS	330	-	-	360	180

32	Jos	330	-	-	141	155
33	Kainji	330	760	313	-	-
34	Kaduna	330	-	-	193	144
35	Kano	330	-	-	180	100
36	Katampe (Abuja)	330	-	-	290	60
37	Lokoja	330	-	-	75	65
38	Makurdi	330	-	-	75	37.7
39	Maiduguri	330	-	-	70	50
40	New Haven	330	-	-	140	10
41	New Haven South	330	-	-	40	27
42	Olorunshogo	330	335	195	-	-
43	Omotosho	330	335	220	-	-
44	Omoku	330	150	75	-	-
45	Oshogbo	330	-	-	201	150
46	Okpai	330	480	330	-	-
47	Onitsha	330	-	-	162	28
48	Owerri	330	-	-	100	60
49	Papalanto	330	1020	450	-	-
50	PortHarcourt	330	200	100	316	159
51	Sapele	330	1020	550	-	-
52	Sakete	330	-	-	145	70
53	Shiroro	330	600	450	-	-
54	Shiroro TS	330	-	-	97.5	22.75
55	Ugwuaji	330	-	-	75.7	46.8
56	Yola	330	-	-	112	65

Table A2. Transmission Line Data (of Bison, two conductors per phase & 2x350 mm² X-section Conductor) for the 330KV Lines obtained from ETAP.

SN	Bus Name		Length (km)	Type of Circuit	R1 (Ω/km)	X1 (Ω/km)	Y1 (μS/km)	R0 (Ω/km)	X0 (Ω/km)	Y0 (μS/km)
	From	To								
1	Afam GS	Alaoji	25	Double	0.01879	0.14976	8.08147	0.17972	1.02342	1.93438
2	Afam GS	Ikot Ekpene	90	Double	0.01879	0.14976	8.08147	0.17972	1.02342	1.93438
3	Afam GS	PortHarcourt	45	Double	0.01879	0.14976	8.08147	0.17972	1.02342	1.93438
4	Ayiède	Oshogbo	115	Single	0.03809	0.033368	3.42768	0.23426	1.09356	1.75899
5	Ayiède	Ikeja West	137	Single	0.03809	0.033368	3.42768	0.23426	1.09356	1.75899
6	Ayiède	Papalanto	60	Single	0.03809	0.033368	3.42768	0.23426	1.09356	1.75899
7	Aja	Egbin PS	14	Double	0.01879	0.14976	8.08147	0.17972	1.02342	1.93438
8	Aja	Alagbon	26	Double	0.01879	0.14976	8.08147	0.17972	1.02342	1.93438
9	Ajaokuta	Benin North	195	Single	0.03809	0.033368	3.42768	0.23426	1.09356	1.75899
10	Ajaokuta	Geregu	5	Double	0.01879	0.14976	8.08147	0.17972	1.02342	1.93438

**INVESTIGATING THE EFFECT OF INTEGRATION OF RENEWABLE POWER PLANTS ON THE NIGERIA
330KV ELECTRICITY GRID**

Martin, et al.

11	Ajaokuta	Lokoja	38	Double	0.01879	0.14976	8.08147	0.17972	1.02342	1.93438
12	Akamgba	Ikeja West	18	Single	0.03809	0.033368	3.42768	0.23426	1.09356	1.75899
13	Aladja	Sapele	63	Single	0.03809	0.033368	3.42768	0.23426	1.09356	1.75899
14	Aladja	Delta PS	32	Single	0.03809	0.033368	3.42768	0.23426	1.09356	1.75899
15	Alaoji	Owerri	60	Double	0.01879	0.14976	8.08147	0.17972	1.02342	1.93438
16	Alaoji	Onitsha	138	Single	0.03809	0.033368	3.42768	0.23426	1.09356	1.75899
17	Alaoji	Ikot Ekpene	38	Double	0.01879	0.14976	8.08147	0.17972	1.02342	1.93438
18	Aliade	New Haven	150	Double	0.01879	0.14976	8.08147	0.17972	1.02342	1.93438
19	Aliade	Makurdi	50	Double	0.01879	0.14976	8.08147	0.17972	1.02342	1.93438
20	B.Kebbi	Kainji	310	Single	0.03809	0.033368	3.42768	0.23426	1.09356	1.75899
21	Benin	Ikeja West	280	Double	0.01879	0.14976	8.08147	0.17972	1.02342	1.93438
22	Benin	Sapele	50	Double	0.01879	0.14976	8.08147	0.17972	1.02342	1.93438
23	Benin	Delta PS	41	Single	0.03809	0.033368	3.42768	0.23426	1.09356	1.75899
24	Benin	Oshogbo	251	Single	0.03809	0.033368	3.42768	0.23426	1.09356	1.75899
25	Benin	Onitsha	137	Single	0.03809	0.033368	3.42768	0.23426	1.09356	1.75899
26	Benin	Benin North	20	Single	0.03809	0.033368	3.42768	0.23426	1.09356	1.75899
27	Benin	Egbin PS	218	Single	0.03809	0.033368	3.42768	0.23426	1.09356	1.75899
28	Benin	Omotosho	51	Single	0.03809	0.033368	3.42768	0.23426	1.09356	1.75899
29	Benin North	Eyaen	5	Double	0.01879	0.14976	8.08147	0.17972	1.02342	1.93438
30	Calabar	Ikot Ekpene	72	Double	0.01879	0.14976	8.08147	0.17972	1.02342	1.93438
31	Damaturu	Gombe	135	Single	0.03809	0.033368	3.42768	0.23426	1.09356	1.75899
32	Damaturu	Maiduguri	140	Single	0.03809	0.033368	3.42768	0.23426	1.09356	1.75899
33	Egbema	Omoku	30	Double	0.01879	0.14976	8.08147	0.17972	1.02342	1.93438
34	Egbema	Owerri	30	Double	0.01879	0.14976	8.08147	0.17972	1.02342	1.93438
35	Egbin PS	Ikeja West	62	Single	0.03809	0.033368	3.42768	0.23426	1.09356	1.75899
36	Egbin PS	Erunkan	30	Single	0.03809	0.033368	3.42768	0.23426	1.09356	1.75899
37	Erunkan	Ikeja West	32	Single	0.03809	0.033368	3.42768	0.23426	1.09356	1.75899
38	Ganmo	Oshogbo	87	Single	0.03809	0.033368	3.42768	0.23426	1.09356	1.75899
39	Ganmo	Jebba TS	80	Single	0.03809	0.033368	3.42768	0.23426	1.09356	1.75899
40	Gombe	Jos	264	Single	0.03809	0.033368	3.42768	0.23426	1.09356	1.75899
41	Gombe	Yola	240	Single	0.03809	0.033368	3.42768	0.23426	1.09356	1.75899
42	Gwagwalada	Lokoja	140	Double	0.01879	0.14976	8.08147	0.17972	1.02342	1.93438
43	Gwagwalada	Shiroro	114	Double	0.01879	0.14976	8.08147	0.17972	1.02342	1.93438
44	Gwagwalada	Katampe	30	Double	0.01879	0.14976	8.08147	0.17972	1.02342	1.93438
45	Ikeja West	Oshogbo	252	Single	0.03809	0.033368	3.42768	0.23426	1.09356	1.75899
46	Ikeja West	Omotosho	200	Single	0.03809	0.033368	3.42768	0.23426	1.09356	1.75899
47	Ikeja West	Papalanto	30	Single	0.03809	0.033368	3.42768	0.23426	1.09356	1.75899
48	Ikeja West	Sakete	70	Single	0.03809	0.033368	3.42768	0.23426	1.09356	1.75899
49	Ikot Abasi	Ikot Ekpene	75	Double	0.01879	0.14976	8.08147	0.17972	1.02342	1.93438
50	Ikot Ekpene	New Haven	143	Double	0.01879	0.14976	8.08147	0.17972	1.02342	1.93438
51	Jalingo	Yola	132	Single	0.03809	0.033368	3.42768	0.23426	1.09356	1.75899
52	Jebba TS	Oshogbo	157	Double	0.01879	0.14976	8.08147	0.17972	1.02342	1.93438
53	Jebba TS	Jebba GS	8	Double	0.01879	0.14976	8.08147	0.17972	1.02342	1.93438
54	Jebba	Kainji	81	Double	0.01879	0.14976	8.08147	0.17972	1.02342	1.93438
55	Jebba	Shiroro	244	Single	0.03809	0.033368	3.42768	0.23426	1.09356	1.75899
56	Jos	Kaduna	196	Single	0.03809	0.033368	3.42768	0.23426	1.09356	1.75899
57	Jos	Makurdi	230	Double	0.01879	0.14976	8.08147	0.17972	1.02342	1.93438
58	Kaduna	Kano	230	Single	0.03809	0.033368	3.42768	0.23426	1.09356	1.75899

59	Kaduna	Shiroro TS	96	Single	0.03809	0.033368	3.42768	0.23426	1.09356	1.75899
60	Abuja (Katampe)	Shiroro GS	144	Double	0.01879	0.14976	8.08147	0.17972	1.02342	1.93438
61	New Haven	Onitsha	96	Single	0.03809	0.033368	3.42768	0.23426	1.09356	1.75899
62	New Haven	New Haven	5	Double	0.01879	0.14976	8.08147	0.17972	1.02342	1.93438
63	Okpai	Onitsha	60	Double	0.01879	0.14976	8.08147	0.17972	1.02342	1.93438
64	Onitsha	Owerri	137	Double	0.01879	0.14976	8.08147	0.17972	1.02342	1.93438

Table A3: Parameters of the PV Module

Description	Parameters	Parameters
Maximum Power at STC (Pmax)	275W	280W
Optimum Operating Voltage (Vmp)	35.1V	35.2V
Optimum Operating Current (Imp)	7.84A	7.95A
Open-Circuit Voltage (Voc)	44.7V	44.8V
Short-Circuit Current (Isc)	8.26A	8.33A
Module Efficiency	14.2%	14.4%
Operating Module Temperature	-40 ⁰ C to +85 ⁰ C	
Maximum System Voltage	600V DC(UL)/1000V DC (IEC)	
Maximum Series Fuse Rating	20A	
Power Tolerance	0/5%	

STC: Irradiance 1000W/m², module temperature 25⁰C, AM=1.5; Best in Class AAA solar simulator (IEC 60904-9) used, power measurement uncertainty is within +/-3%.

Table A4: Parameters of Wind Turbine

WTG number	37 GEV MP
Rated power	275 kW
Total power	10.175 MW
Rotor diameter	32 m
Tower height	55 m
Swept area	804.25m ²
Number of blades	2
Cut in wind speed	3.5 m/s
Cut out wind speed	25 m/s
Tower type:	Tubular